

# Gauge cancellation for electroweak processes and the Gervais-Neveu gauge

Y.J. Feng\* and C.S. Lam†

*Department of Physics, McGill University,  
3600 University St., Montreal, P.Q., Canada H3A 2T8*

## Abstract

A graphical method is developed to study the total or partial cancellation of gauge-dependent (divergence) terms in electroweak theory. The method is used to work out rules in the Gervais-Neveu gauge, whose triple-gauge vertex contains three terms rather than the usual six. This and other features of the gauge lead to an enormous saving of algebraic labor in the actual computations, as will be illustrated explicitly in the tree process  $W^+ + W^- \rightarrow \gamma + \gamma$ .

## 1 Introduction

Standard-Model calculations are beleaguered with gauge problems. The algebra is made unnecessarily complicated because individual Feynman diagrams depend on the gauge chosen, although these gauge-dependent terms must all get cancelled out in the sum. While there is no known way to eliminate this complication, a clever choice of gauge can greatly simplify the ensuing calculations. The purpose of this paper is to discuss ways of doing that in the electroweak theory (EW).

Gauge choices can be made on every Feynman-diagram component connected to a gauge particle. Different gauges differ by a divergence factor, *i.e.*, terms proportional to the momentum of the gauge particle. Gauge-dependent terms are made out of these divergence factors; a study of their cancellation is a study of how such divergences from the various diagrams combine to annihilate one another. The purpose of the previous paper [1] and the present one is to develop a simple technique to study this general problem, and hence a tool to help us decide on the best gauge to use. The simplicity results from our systematic use of the graphical language, thus avoiding the very messy algebra otherwise needed. For QCD a detailed discussion can be found in Refs. [1] and [2].

There are three different components of a Feynman diagram where gauge choices can be made: the gauge propagator, the external gauge-particle wave function, and vertices involving a gauge particle. For QCD the gauge propagator is usually chosen to be in the Feynman gauge. For EW it is either the Feynman gauge or the unitary gauge. As far as external gauge-particle wave function is concerned, enormous simplification can be obtained using the spinor helicity method, originally developed to be used with tree diagrams [3], but with the introduction of the electric-circuit technique [4], super-string [5] or first-quantized [6] formalism, the method can equally be used to compute loop diagrams. The remaining gauge-dependent components are the vertices. For QCD [1], simplifications can often be obtained by avoiding using the ordinary three-gluon vertices containing six terms. In tree diagrams, the simplest vertices available are those in the Gervais-Neveu (GN) gauge [7], where the triple gluon vertex contains only three, rather than six, terms. For one-loop one-particle irreducible  $n$ -gluon diagrams, in some sense the background-field method (BFM) [8] offers the greatest economy. For other processes, or two and more loops, it is not known what the best gauge would be, but it will generally not be the ordinary nor the BFM gauge, simply because a new gauge can be constructed for two-loop gluon self-energy diagrams which gives rise to simpler results than either of those two gauges [2].

For electroweak theory, like in QCD, graphical methods can be used to fix gauges. In particular, one can derive the rules to be used in the GN gauge which we will discuss in Sec. 3, and we shall see that its vertices offer enormous simplifications. A comparison for the savings will be illustrated by using the tree process  $W^+ + W^- \rightarrow \gamma + \gamma$ .

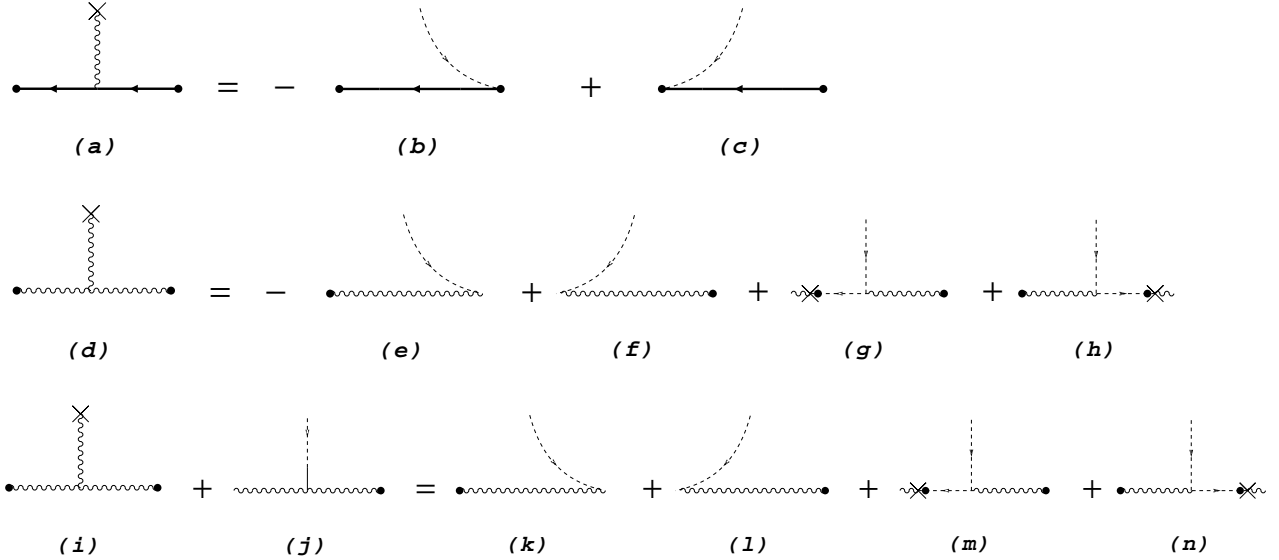


Figure 1: Divergence relations for QED, QCD, and EW. All momenta are outgoing; all particles except the ghost are also outgoing.

This method can also be used to determine how computations can be carried out in other gauges. When applied to obtaining the BFM gauge [9] for one-loop electroweak calculations, we reproduce the results of the pinching technique [10].

## 2 Divergence relations and gauge cancellations

The discussion of gauge transformation and gauge cancellation is necessarily more complicated than the corresponding case in QCD, owing to the following two facts. First the gauge particles ( $g$ ) can now be either  $W^\pm$ ,  $Z$ , or  $\gamma$ , with different masses and different number of polarizations. Secondly, because of spontaneous symmetry breaking, the nonabelian group factor can no longer be isolated. This increases the number of Feynman rules as shown in App. A. Other than these two differences and the associated complications, the discussions are completely parallel to those in QCD [1].

Throughout this paper, we choose Feynman gauge for all the internal propagators, as we did in QCD [1]. We shall focus in the text new aspects appearing in the electroweak theory, leaving other details to the graphical formulas in App. B. As before, we first study the divergences of all the vertices that contain at least one gauge boson ( $g$ ), and then how the various terms so generated are cancelled or partially cancelled.

First let us review the Ward-Takahashi identity in QED. This can be found in many text books [11] on quantum field theory. Graphically, the identity is shown in Figs. 1(a)–1(c). A cross on a gauge boson (wavy) line always denotes the divergence, which is just a factor  $p_\alpha$  for the gauge boson with outgoing momentum  $p$  and Lorentz index  $\alpha$ . A dotted line is a ghost line ( $G$ ). When drawn tangential to a propagator, it simply injects the right amount of momentum into the propagator without changing anything else. This happens in diagrams (b), (c), (e), (f), (k), and (l), which we shall call the *sliding* diagrams. Here and after, each diagram in an identity should be understood as part of a large Feynman diagram. The small dot at the end of a line indicates that its propagator should be included.

The corresponding identity in QCD is shown in Figs. 1(d)–1(h). The complication arising from color source diffusion of a nonabelian theory is reflected in the *propagating* diagrams Figs. 1(g) and 1(h). Here a

cross at the end of a ghost line represents a cross on the gauge-boson line it is connected to. A propagating cross always drags behind it a ghost line, which is a metamorphosis of the gauge-boson line. To distinguish this from an internal ghost line appearing in a loop, this will be called a *wandering ghost line*.

This identity in the case of EW theory (Figs. 1(i)–1(n)) is even more complicated on account of the spontaneous symmetry breaking. This leads to the appearance of the *compensation* diagram (Fig. 1(j)), so called because it compensates the mass difference of those two sliding diagrams. To illustrate this, we write the divergence of a  $WW\gamma$  vertex.

$$\begin{aligned} & (p_2)^\beta T_{\alpha\beta\delta}(p_1, p_2, p_3) + (-iM_W)ieg_{\alpha\delta}M_W \\ = & eg_{\alpha\delta}[-p_3^2 + M_W^2] + eg_{\alpha\delta}[p_1^2] + e(p_1)_\alpha[-(p_1)_\delta] + e(p_3)_\delta[(p_3)_\alpha] . \end{aligned} \quad (1)$$

These terms are shown respectively as Figs. 1(i), 1(j),  $\dots$ , 1(n). A solid line represents a scalar field  $S = \{\phi, H\}$ , where  $\phi$  are the Goldstone fields and  $H$  is the physical Higgs particle. When a ghost line is joined to a solid line  $\phi$  as shown in Fig. 1(j), we assign to the two-point vertex a factor  $-iM_W$ .

Note that we have redefined the sign of the sliding diagram in EW compared to those used in QED and QCD [1]. This simplifies later discussions as will be seen in App. B.

There are many divergence relations shown in App. B. Their general features needed for later discussions will be summarized below.

A divergence relation is an identity with a  $g$ -line crossed in one or two of its vertices. Those diagrams with a cross will be called *divergence diagrams*. If the vertex being crossed does not contain ghost line itself, then there is only one divergence diagram in an identity. If the crossed vertex contains ghost line, then there will be two divergence diagrams (see for example Fig. 18).

We first look at the the divergence relations in App. B with only one divergence diagram. They will be summarized below. By definition, all diagrams carry a coefficient  $+1$ , so it is important to know which of them appear on the lefthand side and which of them appear on the righthand side of the relations.

First the lefthand side of the divergence relations.

Replace the  $g$ -line with a cross by its corresponding  $\phi$ -line. If this new vertex is a legitimate Feynman-rule vertex, then the lefthand side of the relation consists of the divergence diagram as well as a compensation diagram. See for example Figs. 1(i) and 1(j).

Now imagine we remove the crossed  $g$ -line from the divergence diagram. If the new vertex is still a legitimate Feynman-rule vertex, then the lefthand side consists of the divergence diagram as well as sliding diagrams. They are constructed by changing the crossed  $g$ -line into a wandering ghost line. See for example Fig. 16.

Note that only one of these two possibilities occurs in App. B. However, in the GN gauge to be discussed in Sec. 3, both of these possibilities can occur simultaneously. See Fig. 43.

Now the righthand side of the divergence relations.

Propagating diagrams, sliding diagrams, and compensation diagrams appear on the righthand side according to the following rules.

First, if the vertex being crossed is a three point vertex, and if those two uncrossed lines are both  $g$ -lines, fermion lines,  $S$ -lines, or ghost lines, then there are sliding diagrams on the righthand side. For the first three cases, there are two sliding diagrams each with a propagator being cancelled (see for example Fig. 1(k) and 1(l)). For ghost vertex, there is only one sliding diagram with the propagator of the outgoing ghost line being cancelled (see Fig. 19).

Secondly, change the crossed  $g$ -line into an incoming ghost line and any one of the uncrossed  $g$ -lines into an outgoing ghost line. If the new vertex is legitimate, then there is a propagating diagram constructed with this change as shown in Figs. 1(m) and 1(n).

Thirdly, there may be compensation diagram(s) as well, as long as we can legitimately change one of the  $\phi$ -lines in the divergence diagram into an outgoing ghost line, and simultaneously the crossed  $g$ -line into an incoming ghost line (see for example Fig. 12(e)).

Now we are going to look at the divergence relations containing two divergence diagrams on the lefthand side. The diagrams in these identities carry both signs.

In the Feynman gauge, this occurs only in connection with the  $GGg$  vertex – the divergence diagram obtained by interchanging the crossed  $g$ -line with the incoming ghost line has an opposite sign. This can be traced back to the minus sign of the ghost loop.

For either of these two divergence diagrams, we can use the rules discussed before to determine the rest of the diagrams in the relations. See Figs. 19–21.

In the divergence relations, we have included all the possibilities of a cross being placed on any  $g$ -line of a vertex. To complete the list of all the identities, we need to consider relations without crosses. We shall call those *cancellation relations*. They involve diagrams of following two kinds: 1) An incoming ghost line  $G$  is joined to a  $\phi$ -line of a vertex; and 2) A wandering ghost line is tangential to a propagator. Every term below once again has a coefficient +1.

In the first case, if the vertex obtained by replacing the incoming ghost line by a crossed  $g$ -line is legitimate, then the identity has been considered before and is a divergence relation. Otherwise, terms with the  $G - \phi$  line replaced by tangential ghost lines are also present on the lefthand side of the cancellation relation in all possible ways. The righthand side of the identity is zero. See Fig. 24 for an example.

In the second case, we must first decide whether the sliding diagram is already involved in a divergence relation, or an identity under case 1. If not, sum up all the possible sliding diagrams to get zero as the identity. See Fig. 30 for an example.

These are all the identities in Feynman gauge that we need to know.

## 2.1 U(1) gauge symmetry

As an application of these identities, we shall demonstrate explicitly how the remaining  $U(1)$  gauge symmetry is preserved in the diagrammatic language. This means that if we introduce a gauge transformation to one of the external photons,

$$\epsilon^\mu(p) \rightarrow \epsilon^\mu(p) + \lambda p^\mu , \quad (2)$$

with  $\lambda$  being an arbitrary parameter, then the contribution coming from this extra divergence term must sum up to zero, provided all the other external gauge bosons are transversely polarized.

The verification of this is very similar to the case of **R1** considered in QCD [1]. Roughly speaking it is the following. Using the divergence relation on the gauge vertex involving the external photon, propagating, sliding, and compensation diagrams are generated. The crosses in the propagating diagrams can be used in other divergence relations to produce other propagating, sliding, and compensation diagrams, and so on. Whatever sliding or compensation diagrams needed on the lefthand side of a divergence relation will be automatically produced from the last divergence relation. Continuing thus, finally many diagrams are generated for the divergence of the amplitude. The cross is either absent in a diagram, or else it appears in an external  $g$ -line, in which case the corresponding diagram vanishes provided that gauge particle is transversely polarized. The remaining diagrams without crosses sum up to zero by using the cancellation relations. When divergence relations involving two divergence diagrams are used, the argument becomes more complicated because of the presence of the minus signs, but these signs can always be traced back to the signs of the ghost loops so everything will again work out properly. Consequently, just as in QCD [1], we have

- **R1**: The sum of all on-shelled or crossed diagrams with one cross on one of the external photon lines is zero, if all the internal propagators are taken in the Feynman gauge. This is just the remaining  $U(1)$  gauge symmetry.

## 2.2 Equivalence theorem

Another application of these graphical identities is the verification of the equivalence theorem [12]. After spontaneous symmetry breaking, the  $W$  and  $Z$  bosons obtain masses so their external wavefunctions are no longer gauge invariant. From the point of view of the identities in App. B, this lack of invariance is brought about because the corresponding compensation diagram on the left of the divergence relation is now absent.

Since all the longitudinally polarized external wave-function of a massive boson is

$$\frac{1}{M_W}(p, 0, 0, p_0) . \quad (3)$$

Taking the high energy limit

$$E_j \sim k_j \gg M_W, \quad (4)$$

the external wave-function of a W particle can be represented by a cross. This would have produced a zero result at the end if the compensation diagram were present on the lefthand side of the divergence relation. Consequently, longitudinally polarized W boson is equivalent to the corresponding  $\phi$ , which is the content of the equivalence theorem [12].

### 2.3 Pinching technique and Background Field Method

In the previous paper [1] we have shown the affinity between our graphical language and the pinching technique [10] in the case of QCD. The latter can be obtained from the former by changing the vertex to the BFM gauge in the one-loop situation [1, 9]. Now that we have established similar graphical rules for EW, the same connection can be shown in essentially the same way.

## 3 Gervais-Neveu Gauge

The Gervais-Neveu (GN) gauge was first discussed in Ref.[7] for QCD, and for a toy model of massive non-abelian Yang-Mills fields. It was found out later that superstring selects the GN gauge for its QCD tree-level calculations[5]. This is gratifying because in some sense the GN gauge is the simplest gauge to use at the tree level, both for QCD and EW. As a matter of fact, this gauge simplifies computations in the loop levels as well. In this section we shall use the graphical identities to work out the vertices and their Feynman rules in the GN gauge, and we shall discuss a simple example illustrating the amount of labour that can be saved by its use.

To obtain the GN gauge in EW we adopt a procedure very similar to the one used in QCD where the BFM gauge was derived from the Feynman gauge [1]. To avoid a paper with excessive length, we refer the readers to Ref. [1] for most of the details. Nevertheless, we shall summarize the procedure below, with special emphasizes on points that are peculiar to the EW theory.

The Feynman rule for vertices in the GN gauge is not the same as those in the Feynman gauge. In addition, there are new vertices present in the GN gauge. Both of these are summarized in Tables I and II.

The procedure to obtain them can be outlined as follows:

1. By using momentum conservation, the six terms in the usual  $3g$  vertices can be rewritten as the sum of three divergence terms (Figs. 2(c), (d), (e)), and a new GN vertex (Fig. 2(b)), as shown in the formula below:

$$\begin{aligned} & \lambda (g_{\alpha\beta}(p_1 - p_2)_\delta + g_{\beta\delta}(p_2 - p_3)_\alpha + g_{\delta\alpha}(p_3 - p_1)_\beta) \\ = & 2\lambda (g_{\alpha\beta}(p_1)_\delta + g_{\beta\delta}(p_2)_\alpha + g_{\delta\alpha}(p_3)_\beta) + \lambda g_{\alpha\beta}(p_3)_\delta + \lambda g_{\beta\delta}(p_1)_\alpha + \lambda g_{\delta\alpha}(p_2)_\beta, \end{aligned} \quad (5)$$

where  $\lambda = e$  for  $W^+W^-\gamma$  coupling, and  $\lambda = g \cos \theta_W$  for  $W^+W^-Z$  coupling.

2. Results obtained in Secs. 2.1 and 2.2 will be used to show that the three divergence terms combine to cancel one another partially. The remaining terms will combine with other existing vertices to obtain the new vertices shown in Tables I and II.

We shall now discuss in more detail how step 2 above is carried out.

- 2A. Consider all the diagrams containing 2(c), (d), or (e). Imagine for the moment that the incoming ghost line containing the cross is cut open. Apply arguments similar to those used in Secs. 2.1 and 2.2, all diagrams should sum up to be zero if the presence of the external outgoing ghost on the other side of the cut, as well as the subtlety to be mentioned below, are ignored.

The subtlety is the following. In the EW theory there is a distinction between a neutral particle ( $\gamma, Z$ ) and a charged particle ( $W^\pm$ ), in that the compensation diagram is required on the lefthand side of the

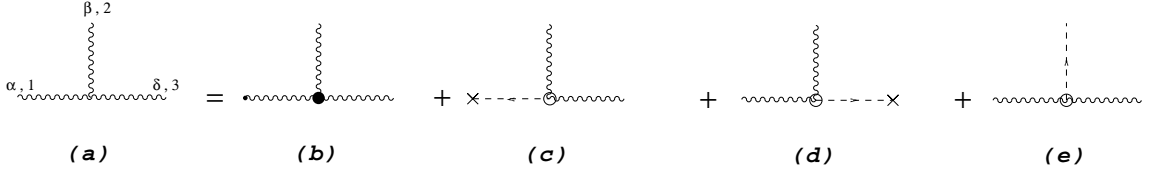


Figure 2: Relation between the  $3g$  vertex in Feynman gauge and in GN gauge. The GN vertex is denoted by a big dot.

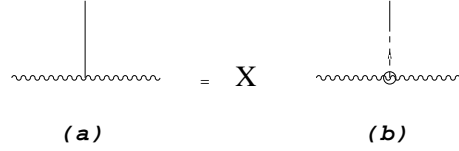


Figure 3: An alternative way to write the  $gg\phi$  vertex.

divergence relations for the latter. The compensation diagram required in the present context must have a ghost line connected to the other side because this is what the crosses in 2(c), (d), and (e) are connected to. For that reason it is convenient to rewrite the  $gg\phi$  vertex in the form of Fig. 3, where  $X = 1$  for  $\gamma(Z)W^-\phi^+$  coupling and  $X = -1$  for  $\gamma(Z)W^+\phi^-$ . If  $X = 1$ , the compensation diagram comes in correctly for the divergence relation to be used. If  $X = -1 = -2 + 1$ , then on top of the compensation diagram, the coefficient of the  $gg\phi$  vertex is now doubled in the GN gauge.

In addition, the actual presence of the outgoing ghost must be taken into account. This gives rise to some ‘leftover terms’ and causes an incomplete cancellation. It is from these leftover terms, combined with other existing vertices, that new vertices and/or new Feynman rules are obtained.

- 2B. The Feynman rule for the  $GGg$  vertex in the GN gauge is obtained from Fig. 4, in which diagram (a) is a leftover term (see 2A). Depending on the sign of the ordinary ghost vertex, the corresponding GN ghost vertex can be either the ‘a-type’:  $(p_1 - p_3)_\beta$ , or the ‘b-type’:  $-(p_3 + p_1)_\beta = (p_2)_\beta$ . The exact result is shown in Table II.
- 2C. There is a new  $GGgg$  vertex created in the GN gauge, obtained from one or two leftover terms as shown in Figs. 5 and 6. Which is which depends on the details and the results are shown in Table II.
- 2D. These GN vertices are obtained diagrammatically by using Fig. 2 for one of the possibly many  $3g$  vertices in the diagram. Once this calculation is completed we will proceed to make the same decomposition for other  $3g$  vertices, one after another. At that point, since there may already be some GN vertices present, in principle new identities are required and still newer vertices can be created. These identities are shown in App. C. The net result is that only one more new vertex is created this way in the GN gauge, which is discussed in the item below.
- 2E. The  $4g$  vertex in the GN gauge shown in Fig. 7(d) is a combination of the usual  $4g$  vertex and some leftover terms. See Table II for the final result.

The final vertex factors for GN gauge is given in the following tables. Here we just list the new vertices and the ones that are different from the ones in Feynman gauge.

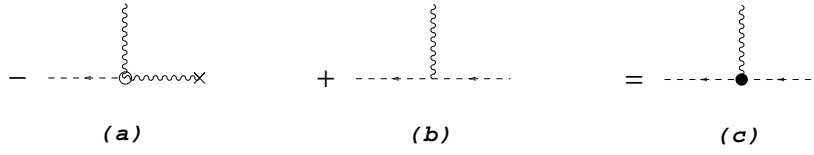


Figure 4: The combination that generates the  $gGG$  vertex in the GN gauge.

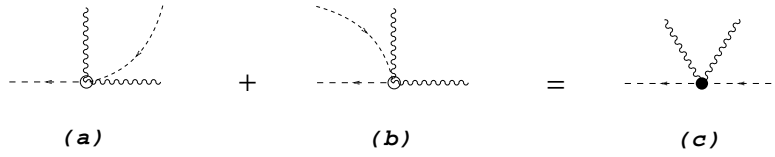


Figure 5: The generation of one kind of  $GGgg$  vertices in the GN gauge.

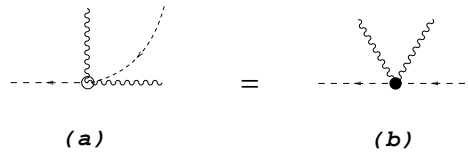


Figure 6: The generation of the other kind of  $GGgg$  vertices in GN gauge.

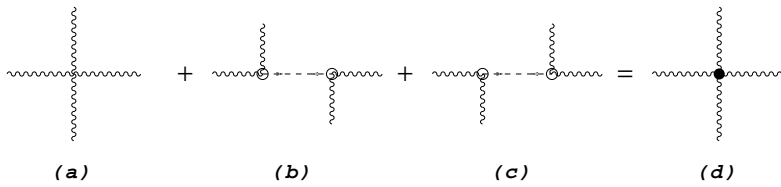


Figure 7: The generation of  $4g$  vertex in GN gauge.

Table for three-point vertices			
1 ( $\alpha$ )	2 ( $\beta$ )	3 ( $\delta$ )	vertex factor
$\phi^+$	$\gamma, Z$	$W^-$	0
$W^+$	$\gamma$	$W^-$	$2e(g^{\alpha\beta}p_1^\delta + g^{\beta\delta}p_2^\alpha + g^{\delta\alpha}p_3^\beta)$
$W^+$	$Z$	$W^-$	$2g \cos \theta_W (g^{\alpha\beta}p_1^\delta + g^{\beta\delta}p_2^\alpha + g^{\delta\alpha}p_3^\beta)$
$W^+$	$\gamma$	$\phi^-$	$2ieM_W g^{\beta\delta}$
$W^+$	$\phi_z$	$W^-$	$ig \cos \theta_W M_z g^{\alpha\delta}$
$W^+$	$Z$	$\phi^-$	$-2ig \sin^2 \theta_W M_z g^{\alpha\beta}$
$\bar{c}^-$	$W^+$	$c_{\gamma,z}$	$e(p_1 - p_3)_\beta, g \cos \theta_W (p_1 - p_3)_\beta$
$\bar{c}^+$	$\gamma, Z$	$c^-$	$e(p_1 - p_3)_\beta, g \cos \theta_W (p_1 - p_3)_\beta$
$\bar{c}_{\gamma,z}$	$W^-$	$W^+$	$e(p_1 - p_3)_\beta, g \cos \theta_W (p_1 - p_3)_\beta$
$\bar{c}^+$	$W^-$	$c_{\gamma,z}$	$-e(p_1 + p_3)_\beta, -g \cos \theta_W (p_1 + p_3)_\beta$
$\bar{c}^-$	$\gamma, Z$	$c^+$	$-e(p_1 + p_3)_\beta, -g \cos \theta_W (p_1 + p_3)_\beta$
$\bar{c}_{\gamma,z}$	$W^+$	$c^-$	$-e(p_1 + p_3)_\beta, -g \cos \theta_W (p_1 + p_3)_\beta$

Table I

Table for four-point vertices				
1 ( $\alpha$ )	2 ( $\beta$ )	3 ( $\delta$ )	4 ( $\rho$ )	vertex factor
$W^+$	$W^+$	$W^-$	$W^-$	$g^2(2g^{\alpha\beta}g^{\delta\rho})$
$W^+$	$\gamma$	$\gamma$	$W^-$	$e^2(-2g^{\alpha\rho}g^{\beta\delta} + 2g^{\alpha\delta}g^{\beta\rho} + 2g^{\alpha\beta}g^{\rho\delta})$
$W^+$	$Z$	$Z$	$W^-$	$g^2 \cos^2 \theta_W (-2g^{\alpha\rho}g^{\beta\delta} + 2g^{\alpha\delta}g^{\beta\rho} + 2g^{\alpha\beta}g^{\rho\delta})$
$W^+$	$\gamma$	$Z$	$W^-$	$eg \cos \theta_W (-2g^{\alpha\rho}g^{\beta\delta} + 2g^{\alpha\delta}g^{\beta\rho} + 2g^{\alpha\beta}g^{\rho\delta})$
$\bar{c}^+$	$W^-$	$W^-$	$c^+$	$-2g^2g^{\beta\delta}$
$\bar{c}^-$	$W^+$	$W^+$	$c^-$	$2g^2g^{\beta\delta}$
$\bar{c}^-$	$W^-$	$W^+$	$c^+$	$-g^2g^{\beta\delta}$
$\bar{c}^+$	$W^+$	$W^-$	$c^-$	$g^2g^{\beta\delta}$
$\bar{c}_\gamma$	$W^+$	$\gamma$	$c^-$	$-e^2g^{\beta\delta}$
$\bar{c}_\gamma$	$W^-$	$\gamma$	$c^+$	$e^2g^{\beta\delta}$
$\bar{c}^-$	$W^+$	$\gamma$	$c_\gamma$	$-e^2g^{\beta\delta}$
$\bar{c}^+$	$W^-$	$\gamma$	$c_\gamma$	$e^2g^{\beta\delta}$
$\bar{c}^+$	$\gamma$	$\gamma$	$c^-$	$-2e^2g^{\beta\delta}$
$\bar{c}^-$	$\gamma$	$\gamma$	$c^+$	$2e^2g^{\beta\delta}$
$\bar{c}_z$	$W^+$	$Z$	$c^-$	$-g^2 \cos^2 \theta_W g^{\beta\delta}$
$\bar{c}_z$	$W^-$	$Z$	$c^+$	$g^2 \cos^2 \theta_W g^{\beta\delta}$
$\bar{c}^-$	$W^+$	$Z$	$c_z$	$-g^2 \cos^2 \theta_W g^{\beta\delta}$
$\bar{c}^+$	$W^-$	$Z$	$c_z$	$g^2 \cos^2 \theta_W g^{\beta\delta}$
$\bar{c}^+$	$Z$	$Z$	$c^-$	$2g^2 \cos^2 \theta_W g^{\beta\delta}$
$\bar{c}^+$	$Z$	$Z$	$c^+$	$-2g^2 \cos^2 \theta_W g^{\beta\delta}$
$\bar{c}_z$	$W^+$	$\gamma$	$c^-$	$-eg \cos \theta_W g^{\beta\delta}$
$\bar{c}_z$	$W^-$	$\gamma$	$c^+$	$eg \cos \theta_W g^{\beta\delta}$
$\bar{c}^-$	$W^+$	$\gamma$	$c_z$	$-eg \cos \theta_W g^{\beta\delta}$
$\bar{c}^+$	$W^-$	$\gamma$	$c_z$	$eg \cos \theta_W g^{\beta\delta}$
$\bar{c}_\gamma$	$W^+$	$Z$	$c^-$	$-eg \cos \theta_W g^{\beta\delta}$
$\bar{c}_\gamma$	$W^-$	$Z$	$c^+$	$eg \cos \theta_W g^{\beta\delta}$
$\bar{c}^-$	$W^+$	$Z$	$\gamma$	$-eg \cos \theta_W g^{\beta\delta}$
$\bar{c}^+$	$W^-$	$Z$	$\gamma$	$eg \cos \theta_W g^{\beta\delta}$
$\bar{c}^+$	$\gamma$	$Z$	$c^-$	$-2eg \cos \theta_W g^{\beta\delta}$
$\bar{c}^-$	$\gamma$	$Z$	$c^+$	$2eg \cos \theta_W g^{\beta\delta}$

Table II



### 3.1 An example of $W^+W^- \rightarrow \gamma\gamma$

The computational simplification by using the GN vertices results mainly from two sources. First and foremost, each  $3g$  vertex gets reduced from six terms to three terms. Secondly, the vanishing vertex appearing in the first line of Table II means that charged-scalar exchange will never occur in tree diagrams in spite of Feynman propagators being used. The combination of these two and other minor effects results in enormous simplification of the algebra.

To illustrate the simplification, we have computed the tree diagrams for  $W^+ + W^- \rightarrow \gamma + \gamma$  in different gauges. The total number of terms in the unitary, Feynman, and GN gauges are respectively 147, 77, and 21. Using *Mathematica*<sup>R</sup> to compute, the total time needed for each of these three cases turns out to be 8.69, 2.13, and 0.52 seconds.

Gauge	Time	Number of terms
Feynman	2.13s	77
unitary	8.69s	147
GN	0.52s	21

Table III

## 4 Conclusion

In this paper we have shown how to carry out gauge transformation graphically in the EW theory. The idea and procedure are fairly similar to those used previously for QCD [1], but the presence of spontaneously symmetry breaking complicates matter and makes the analysis much longer. Using these graphical rules, new gauges not accessible to the operator or path-integral approach can be contemplated. Gauges can now be designed differently for different sets of Feynman diagrams to maximize the reduction of the algebra caused by the gauge-dependent terms. As an illustration of the graphical rules, we worked out the Gervais-Neveu gauge in the EW theory, and applied it to calculate the tree process  $W^+ + W^- \rightarrow \gamma + \gamma$ . The computation in the GN gauge is a factor of 4 faster than in the Feynman gauge, and a factor of 17 faster than in the unitary gauge.

## 5 Acknowledgement

This research was supported in part by the Natural Science and Engineering Research Council of Canada and by the Québec Department of Education. Y.J.F. acknowledges the support of the Carl Reinhardt Major Foundation.

## A Feynman rules in Electroweak theory

	$[g \cos \theta_W] \left( (k-p)^\delta g^{\alpha\beta} + (p-q)^\alpha g^{\beta\delta} + (q-k)^\beta g^{\alpha\delta} \right)$
	$[e] \left( (k-p)^\delta g^{\alpha\beta} + (p-q)^\alpha g^{\beta\delta} + (q-k)^\beta g^{\alpha\delta} \right)$
	$e^2 (g^{\alpha\rho} g^{\beta\delta} + g^{\alpha\delta} g^{\beta\rho} - 2g^{\alpha\beta} g^{\rho\delta})$
	$eg \cos \theta_W (g^{\alpha\rho} g^{\beta\delta} + g^{\alpha\delta} g^{\beta\rho} - 2g^{\alpha\beta} g^{\rho\delta})$
	$g^2 \cos^2 \theta_W (g^{\alpha\rho} g^{\beta\delta} + g^{\alpha\delta} g^{\beta\rho} - 2g^{\alpha\beta} g^{\rho\delta})$
	$-g^2 (g^{\alpha\rho} g^{\beta\delta} + g^{\alpha\beta} g^{\rho\delta} - 2g^{\alpha\delta} g^{\beta\rho})$
	$-\frac{g}{2 \cos \theta_W} \gamma_\alpha \left( \frac{1}{2} - 2Q_i \sin^2 \theta_W - \frac{1}{2} \gamma_5 \right)$
	$\frac{g}{2 \cos \theta_W} \gamma_\alpha \left( \frac{1}{2} - 2Q_I \sin^2 \theta_W - \frac{1}{2} \gamma_5 \right)$
	$eQ_n \gamma_\alpha \quad (n = i, I)$
	$\frac{g}{2\sqrt{2}} \gamma_\alpha U_{iI}^* (1 - \gamma_5)$
	$\frac{g}{2\sqrt{2}} \gamma_\alpha U_{iI} (1 - \gamma_5)$
	$\left[ \frac{i g}{2} \right] (q-p)_\alpha$
	$\left[ \frac{i g}{2} \right] (q-p)_\alpha$
	$\left[ \frac{g}{2} \right] (q-p)_\alpha$
	$\left[ \frac{g}{2} \right] (p-q)_\alpha$
	$\left[ \frac{g}{2 \cos \theta_W} \right] (1 - 2 \cos^2 \theta_W) (q-p)_\alpha$
	$[e] (p-q)_\alpha$
	$\left[ \frac{i g}{\cos \theta_W} \right] (q-p)_\alpha$

	$gM_W g^{\alpha\beta}$		$2e^2 g^{\alpha\beta}$
	$\frac{gM_Z}{\cos\theta_W} g^{\alpha\beta}$		$\frac{g^2}{2} g^{\alpha\beta}$
	$ieM_Z \sin\theta_W g^{\alpha\beta}$		$\frac{eg(2\sin^2\theta_W - 1)}{\cos\theta_W} g^{\alpha\beta}$
	$-ieM_W g^{\alpha\beta}$		$\frac{(2\sin^2\theta_W - 1)g^2}{2\cos^2\theta_W} g^{\alpha\beta}$
	$-ieM_Z \sin\theta_W g^{\alpha\beta}$		$-\frac{eg}{2} g^{\alpha\beta}$
	$ieM_W g^{\alpha\beta}$		$-\frac{3gM_H^2}{2M_Z \cos\theta_W}$
	$-\frac{eg}{2} g^{\alpha\beta}$		$-\frac{gM_H^2}{2M_Z \cos\theta_W}$
	$\frac{e^2}{\cos\theta_W} g^{\alpha\beta}$		$-\frac{gM_H^2}{2M_Z \cos\theta_W} g^{\alpha\beta}$
	$\frac{e^2}{\cos\theta_W} g^{\alpha\beta}$		$-\frac{3g^2 M_H^2}{4M_Z^2 \cos^2\theta_W}$
	$\frac{g^2}{\cos^2\theta_W} g^{\alpha\beta}$		$-\frac{3g^2 M_H^2}{4M_Z^2 \cos^2\theta_W}$
	$\frac{g^2}{2} g^{\alpha\beta}$		$-\frac{g^2 M_H^2}{4M_Z^2 \cos^2\theta_W}$
	$\frac{ig^2}{2} g^{\alpha\beta}$		$-\frac{g^2 M_H^2}{4M_Z^2 \cos^2\theta_W}$
	$-\frac{ig^2}{2} g^{\alpha\beta}$		$-\frac{g^2 M_H^2}{4M_Z^2 \cos^2\theta_W}$
	$-\frac{ie^2}{2\cos\theta_W} g^{\alpha\beta}$		$-\frac{g^2 M_H^2}{2M_Z^2 \cos^2\theta_W}$
	$\frac{ie^2}{2\cos\theta_W} g^{\alpha\beta}$		$\frac{ig}{2} M_Z (2\cos^2\theta_W - 1)$
	$\frac{g^2}{2\cos^2\theta_W} g^{\alpha\beta}$		$ieM_W$
	$\frac{g^2}{2} g^{\alpha\beta}$		$-i\frac{g}{2} M_Z$

	$-\frac{g}{2}M_W$		$[g \cos \theta_W]p_\alpha$
	$-\frac{g}{2 \cos \theta_W}M_z$		$-[g \cos \theta_W]p_\alpha$
	$\frac{ig}{2}M_W$		$-[e]p_\alpha$
	$-\frac{ig}{2}M_W$		$[e]p_\alpha$
	$-ieM_W$		$-[g \cos \theta_W]p_\alpha$
	$i\frac{g}{2}M_z$		$[g \cos \theta_W]p_\alpha$
	$-i\frac{g}{2}M_z(2 \cos^2 \theta_W - 1)$		$-[e]p_\alpha$
	$-\frac{g}{2}M_W$		$[e]p_\alpha$
	$i\frac{g}{2M_W}m_i$		
	$i\frac{g}{2M_W}m_I$		
	$-i\frac{g}{2M_W}m_n \quad (n = i, I)$		
	$-i\frac{g}{2\sqrt{2}M_W}U_{iI}((m_i - m_I) + (m_i + m_I)\gamma_5)$		
	$-i\frac{g}{2\sqrt{2}M_W}U_{iI}^*((m_I - m_i) + (m_i + m_I)\gamma_5)$		
	$[e]p_\alpha$		
	$-[e]p_\alpha$		
	$[g \cos \theta_W]p_\alpha$		
	$-[g \cos \theta_W]p_\alpha$		

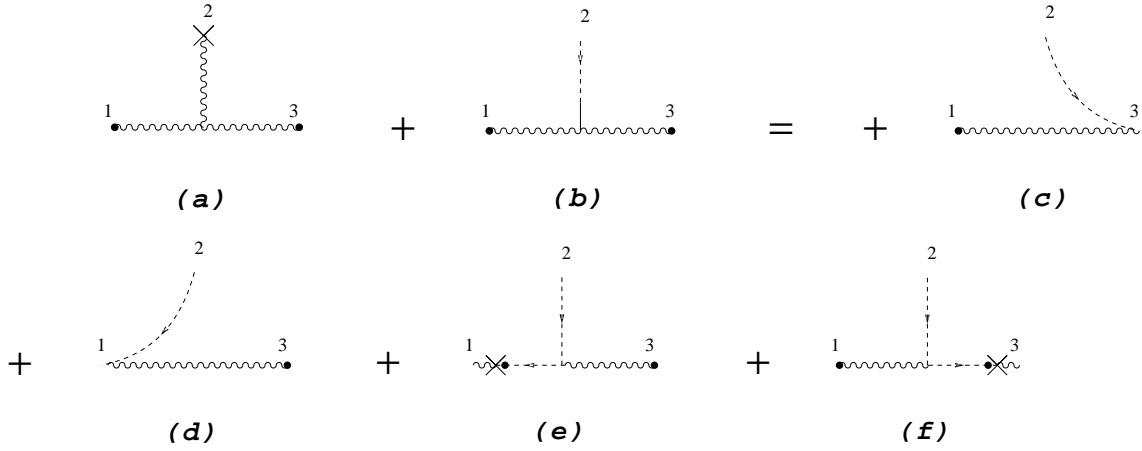


Figure 8: Divergence relation of the triple gauge boson vertex. If line 2 is a photon line or  $Z$ , then (b) is absent.

## B Divergence relations and cancellations

This appendix deals with all the graphical identities in the Feynman gauge. Those involving fermions can be obtained similarly but will not be explicitly discussed here. Wavy, dotted, solid lines are gauge, ghost, and scalar fields respectively, and a cross represents a divergence. Moreover,

1. When a ghost line is connected to its unphysical scalar, a factor  $-iM$  is assigned to the two-point vertex, where  $M$  is the mass of the corresponding gauge particle.
2. The sign and the numerical factor for a sliding diagram is determined as follows. The numerical factor is given by the ‘coupling constant’ of the three-point vertex where the sliding diagram comes from. By ‘coupling constant’, one means the numerical factor at the vertex in App. A enclosed in a square bracket  $[\dots]$ . The sign is determined as follows. First, for vertices not involving a ghost, a standard clockwise orientation is established for each of them. They are, in clockwise orders,  $W^-W^+\gamma(Z)$ ,  $\phi^\pm W^\mp H$ ,  $\phi^+W^-\phi_z$ ,  $\phi_zW^+\phi^-$ ,  $\phi^+Z\phi^-$ ,  $\phi^-\gamma\phi^+$ , and  $\phi_zZH$ . If the wandering ghost line turns to the left along the direction of its arrow, then the sign is negative; if it turns to the right, then the sign is positive. For vertices involving ghost lines, there is only one sliding diagram per vertex, then the sign is positive for the vertices  $\bar{G}_W W^- G_z$ ,  $\bar{G}_W W^- G_\gamma$ ,  $\bar{G}_z W^+ G_W$ ,  $\bar{G}_\gamma W^+ G_W$ ,  $\bar{G}_W \gamma G_{W^+}$ ,  $\bar{G}_W Z G_{W^+}$ , and negative for the vertices  $\bar{G}_W W^+ G_z$ ,  $\bar{G}_W W^+ G_\gamma$ ,  $\bar{G}_z W^- G_W$ ,  $\bar{G}_\gamma W^- G_W$ ,  $\bar{G}_W \gamma G_{W^-}$ ,  $\bar{G}_W Z G_{W^-}$ .

### B.1 Divergence relations

1. ggg:

The relation is shown in Fig. 8.

2. ggS:

There are several cases.

(a)  $W\gamma\phi$  with the cross on the  $\gamma$  line, and  $WZ\phi$  with the cross on the  $Z$  line are shown in Fig. 9.

(b)  $W\gamma\phi$  with the cross on the  $W$  line. It is shown in Fig. 10 with 10(d) absent.

(c)  $WWH$  and  $ZZH$  vertices. The situations here are the same as in Fig. 10 with 10(c) absent.

3. gSS: Because of the presence of the problem of mass compensation, we have to discuss them separately.

(a)  $Z\phi\phi$  and  $\gamma\phi\phi$ . All of them are similar to the scalar QED case, and they are shown in Fig. 11.

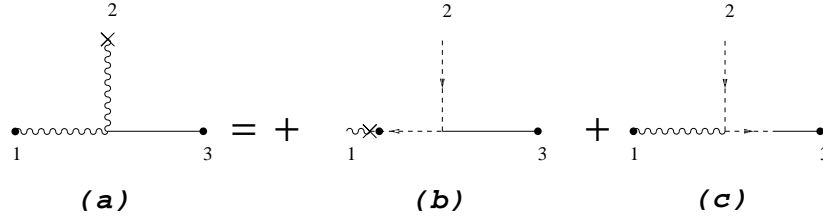


Figure 9: Divergence relation of  $ggS$ .

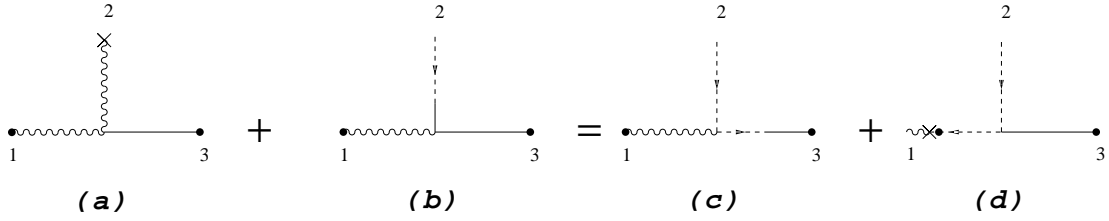


Figure 10: The crossed line in (a) is a  $W$  particle.

(b)  $g\phi H$ : The  $W$  line can be either an outgoing  $W^-$  or an outgoing  $W^+$ . We use Fig. 12 to cover these two possibilities by choosing the following convention. If the cross is on an outgoing  $W^+$ , we use line 1 to represent the Higgs. If the cross is on an outgoing  $W^-$ , we choose line 3 to be the Higgs.

(c)  $g\phi\phi_z$ : The ghost now can turn to either of the scalar lines as shown in Fig. 13.

4.  $gggg$ :

All the cases can be represented by one identity as shown in Fig. 14.

5.  $ggSS$ :

There are three possibilities here: the boson can slide along  $gS$ ,  $SS$ ,  $gSS$ .

(a)  $gS$ : They include  $W\gamma H\phi$ ,  $W\gamma\phi\phi_z$ ,  $WW\phi\phi$ ,  $ZZ\phi\phi$ ,  $\gamma\gamma\phi\phi$ , and  $\gamma Z\phi\phi$ . This is shown in Fig. 15.

(b)  $SS$ : They include  $WWHH$ ,  $ZZHH$ ,  $WW\phi_z\phi_z$ , and  $ZZ\phi_z\phi_z$ . We use Fig. 16 to show them.

(c)  $gSS$ : They include  $WZH\phi$ , and  $WZ\phi\phi_z$ . We use Fig. 17 to show them.

6.  $gGG$ :

The number of compensation diagrams on the left varies:

(a) For vertices  $W\bar{G}_\phi G_z$ ,  $Z\bar{G}_\phi G_\phi$ , and  $W\bar{G}_z G_\phi$ , there are two compensation diagrams as shown in Fig. 18.

(b) For vertices  $W\bar{G}_\phi G_\gamma$ , and  $\gamma\bar{G}_\phi G_\phi$ , there is one compensation diagram as shown in Fig. 19.

(c) For the vertex  $W\bar{G}_\gamma G_\phi$ , there is no compensation diagram as shown in Fig. 20.

These are all the divergence relations in Feynman gauge.

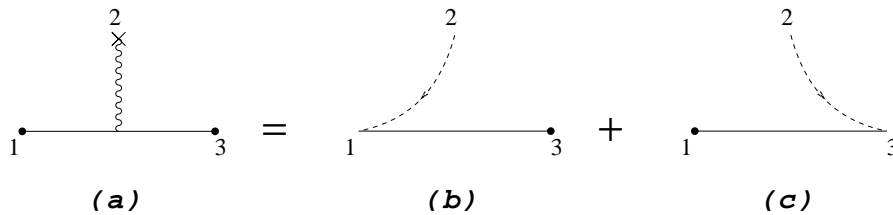


Figure 11: The divergence relation of  $gSS$  vertex.

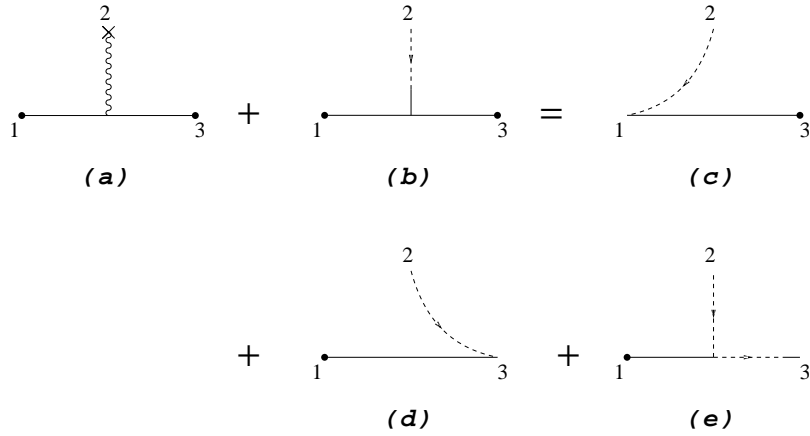


Figure 12: Another divergence relation of the  $gSS$  vertex.

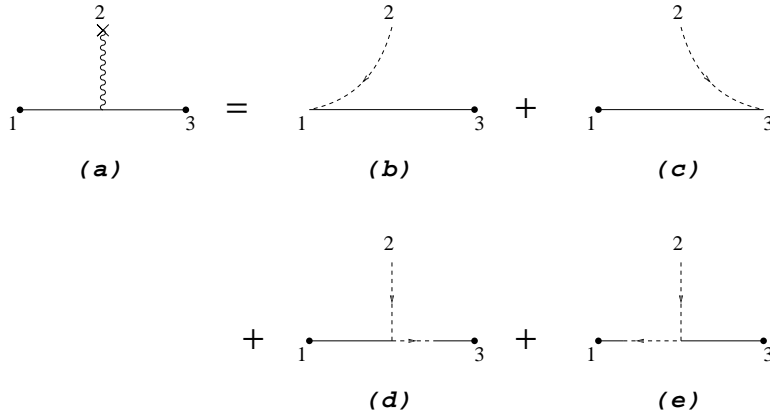


Figure 13: Divergence relation of  $gSS$  vertex again.

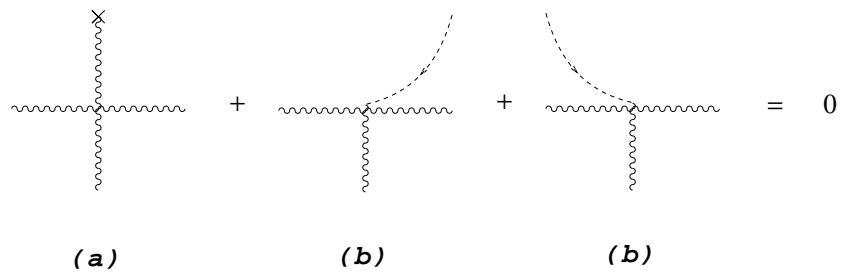


Figure 14: The divergence relation for  $gggg$  vertex.

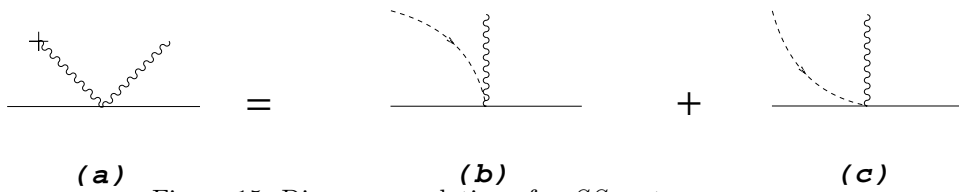


Figure 15: Divergence relation of  $ggSS$  vertex.

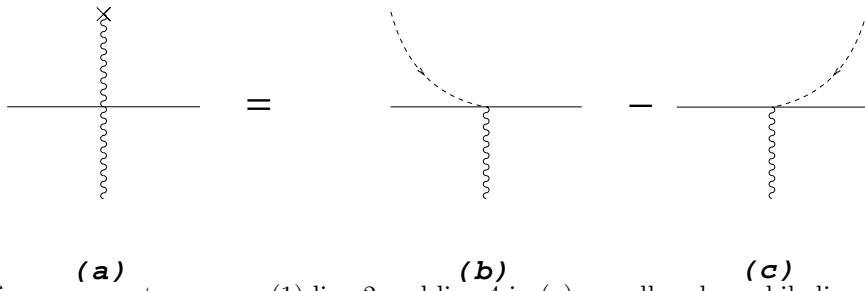


Figure 16: This figure covers two cases: (1) line 2 and line 4 in (a) are all scalar, while line 1 and line 3 are Higgs. (2) All of them are scalar while line 1 and line 3 have the same charge.

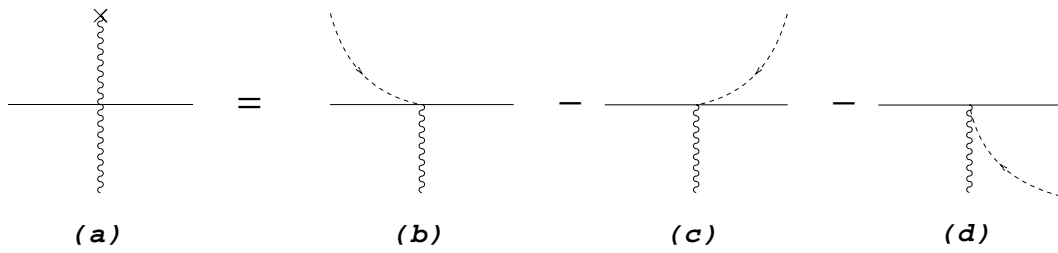


Figure 17: Divergence relation of  $ggSS$  vertex.

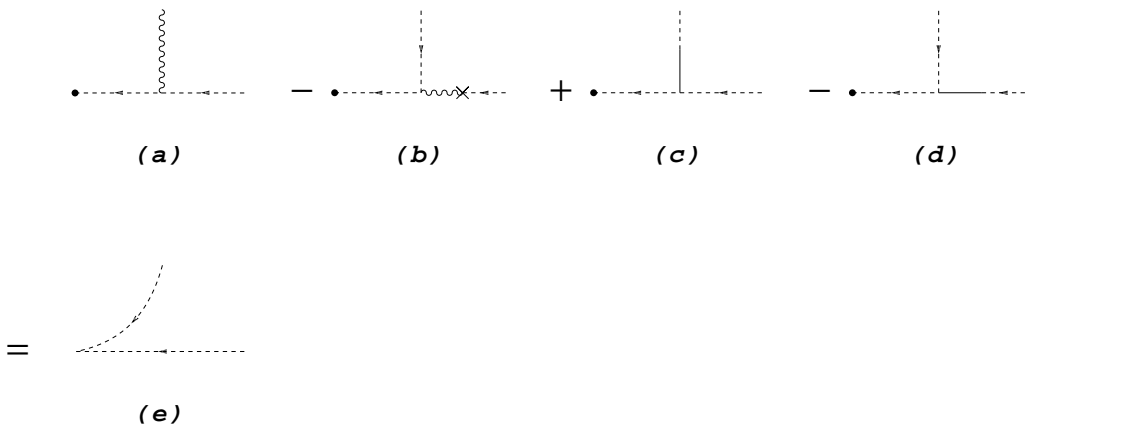


Figure 18: Divergence relation of  $gGG$  vertex.

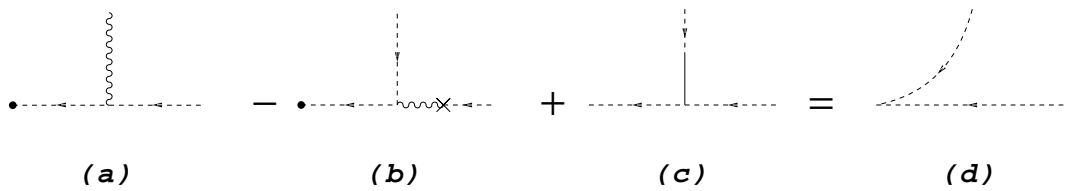


Figure 19: Divergence relation of the  $gGG$  vertex.



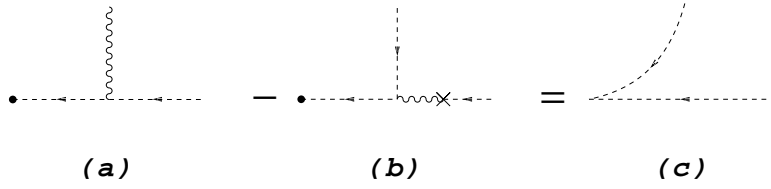


Figure 20: Divergence relation of the  $gGG$  vertex.

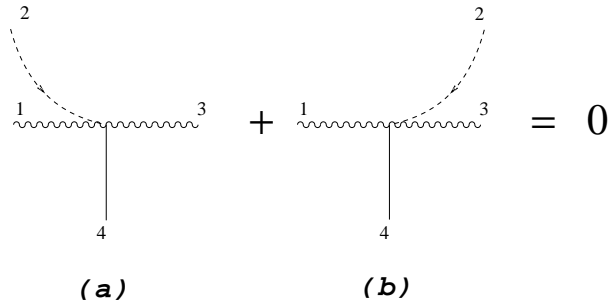


Figure 21: Cancellation relation of the  $ggS$  vertex.

## B.2 Cancellation of the sliding diagrams

1.  $ggg$  vertices: They are the same as in QCD diagrams.
2.  $ggS$  vertices: The various cases are summarized in the following table and Figs. 21 to 24.

Vertex	sliding line	figure	1	2	3	4
$HWW$	$\gamma, Z$	Fig. 21	$W$	$\gamma, Z$	$W$	$H$
$HZZ, \phi WZ$	$W$	Fig. 22	$Z$	$H$	$W$	$W$
$W^\pm Z(\gamma)\phi^\mp$	$\gamma$	Fig. 23	$W$	$Z$	$\phi$	$\gamma$
	$Z$	Fig. 24	$W$	$Z$	$\phi$	$Z$
	$W^\mp$	Fig. 23	$W^\pm$	$W^\pm$	$\phi^\mp$	$W^\mp$

3.  $ggSS$  vertices: The various cases are summarized in the following table and Figs. 25 to 30.

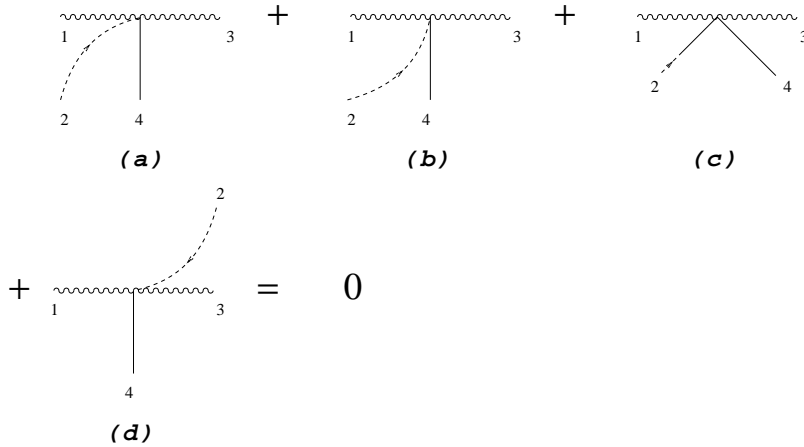


Figure 22: Cancellation relation of the  $ggS$  vertex.

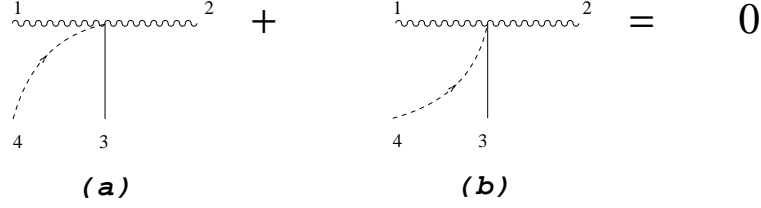


Figure 23: Cancellation relation of the  $ggS$  vertex.

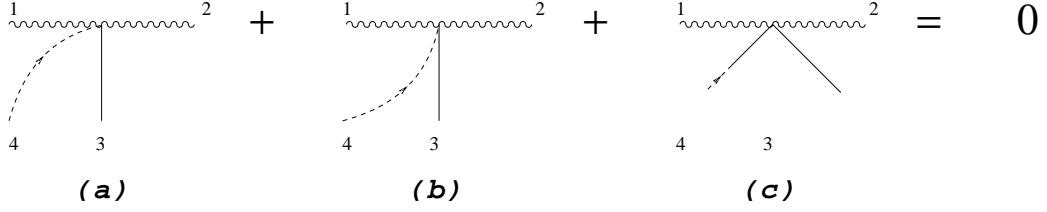


Figure 24: Cancellation relation of the  $ggS$  vertex.

vertex	sliding line	figure	1	2	3	4
$HHWW$	$\gamma, Z$	Fig. 25	$H$	$W$	$W$	$H$
	$Z$	Fig. 27	$H$	$W$	$W$	$\phi$
	$W$	Fig. 29	$H$	$W$	$W$	$\phi$
$HHZZ$	$W$	Fig. 30	$H$	$Z$	$W$	$H$
$H\phi WZ$	$\gamma$	Fig. 26	$H$	$Z$	$W$	$\phi$
	$Z$	Fig. 29	$H$	$W$	$Z$	$\phi$
	$W$	Fig. 29	$H$	$W$	$W$	$\phi$
	$W^\pm$	Fig. 25	$H$	$W^\mp$	$W^\mp$	$\phi^\pm$
$HW\gamma\phi$	$\gamma$	Fig. 26	$H$	$\gamma$	$W$	$\phi$
	$Z$	Fig. 29	$H$	$W$	$\gamma$	$\phi$
$WW\phi_z\phi_z$	$\gamma, Z$	Fig. 25	$\phi_z$	$W$	$W$	$\phi_z$
	$W^\pm$	Fig. 29	$\phi$	$W^\mp$	$W^\pm$	$\phi_z$
$ZZ\phi_z\phi_z$	$W^\pm$	Fig. 30	$\phi_z$	$W^\mp$	$Z$	$\phi_z$
$WZ\phi\phi_z$	$\gamma$	Fig. 26	$\phi_z$	$Z$	$W$	$\phi$
	$Z$	Fig. 29	$\phi_z$	$W$	$Z$	$\phi$
	$W^\pm$	Fig. 25	$\phi_z$	$W^\mp$	$W^\mp$	$\phi^\pm$
$W\gamma\phi\phi_z$	$\gamma$	Fig. 26	$\phi_z$	$\gamma$	$W$	$\phi$
	$Z$	Fig. 29	$\phi_z$	$W$	$\gamma$	$\phi$
$WW\phi\phi$	$\gamma, Z$	Fig. 30	$\phi$	$W$	$W$	$\phi$
$ZZ\phi\phi$	$\gamma, Z$	Fig. 27	$\phi$	$Z$	$Z$	$\phi$
	$W$	Fig. 28	$\phi$	$W$	$Z$	$\phi$
$\gamma\gamma\phi\phi$	$\gamma, Z$	Fig. 27	$\phi$	$\gamma$	$\gamma$	$\phi$
	$W$	Fig. 29	$\phi$	$\gamma$	$W$	$\phi$
$\gamma Z\phi\phi$	$\gamma, Z$	Fig. 27	$\phi$	$\gamma$	$Z$	$\phi$

4.  $gSS$  vertices: They have already been discussed in Fig. 15, Fig. 16, and Fig. 17.

5.  $gggg$ :

There are several cases:

vertex	sliding line	figure	line 1	line 2	line 3	line 4
$W(\gamma, Z)WWW(\gamma, Z)$	$\gamma(Z)$	Fig. 31	$W^+(\gamma, Z)$	$W^+$	$W^-$	$W^-(\gamma, Z)$
$WWWW(WW\gamma(Z)\gamma(Z))$	$W^\pm$	Fig. 32	$\gamma(Z)$	$W^\mp$	$W^\mp$	$W^\pm$

$$\begin{array}{c}
 \begin{array}{ccc}
 & 5 & \\
 & \text{---} & \\
 2 & & 3 \\
 \text{---} & & \text{---} \\
 1 & & 4
 \end{array}
 + 
 \begin{array}{ccc}
 & 5 & \\
 & \text{---} & \\
 2 & & 3 \\
 \text{---} & & \text{---} \\
 1 & & 4
 \end{array}
 = 0 \\
 \text{(a)} \qquad \qquad \qquad \text{(b)}
 \end{array}$$

Figure 25: Cancellation relation of the  $ggSS$  vertex.

$$\begin{array}{c}
 \begin{array}{ccc}
 & 5 & \\
 & \text{---} & \\
 2 & & 3 \\
 \text{---} & & \text{---} \\
 1 & & 4
 \end{array}
 + 
 \begin{array}{ccc}
 & & \\
 & & \text{---} \\
 2 & & 3 \\
 \text{---} & & \text{---} \\
 1 & & 4
 \end{array}
 = 0 \\
 \text{(a)} \qquad \qquad \qquad \text{(b)}
 \end{array}$$

Figure 26: Cancellation relation of the  $ggSS$  vertex.

$$\begin{array}{c}
 \begin{array}{ccc}
 & & \\
 & & \text{---} \\
 2 & & 3 \\
 \text{---} & & \text{---} \\
 1 & & 4
 \end{array}
 + 
 \begin{array}{ccc}
 & & \\
 & & \text{---} \\
 2 & & 3 \\
 \text{---} & & \text{---} \\
 1 & & 4
 \end{array}
 = 0 \\
 \text{(a)} \qquad \qquad \qquad \text{(b)}
 \end{array}$$

Figure 27: Cancellation relation of the  $ggSS$  vertex.

$$\begin{array}{c}
 \begin{array}{ccc}
 & 5 & \\
 & \text{---} & \\
 2 & & 3 \\
 \text{---} & & \text{---} \\
 1 & & 4
 \end{array}
 + 
 \begin{array}{ccc}
 & 5 & \\
 & \text{---} & \\
 2 & & 3 \\
 \text{---} & & \text{---} \\
 1 & & 4
 \end{array}
 + 
 \begin{array}{ccc}
 & & \\
 & & \text{---} \\
 2 & & 3 \\
 \text{---} & & \text{---} \\
 1 & & 4
 \end{array}
 = 0 \\
 \text{(a)} \qquad \qquad \qquad \text{(b)} \qquad \qquad \qquad \text{(c)}
 \end{array}$$

Figure 28: Cancellation relation of the  $ggSS$  vertex.

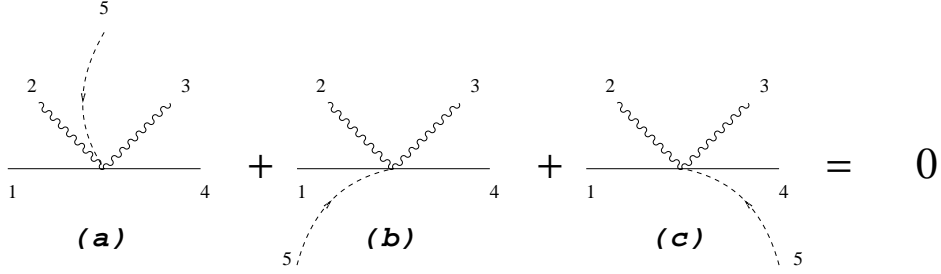


Figure 29: Cancellation relation of the  $ggSS$  vertex.

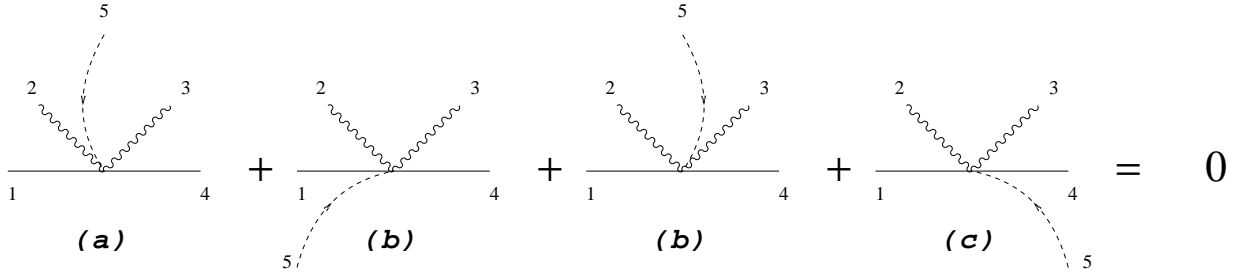


Figure 30: Cancellation relation of the  $ggSS$  vertex.

6. SSS vertices: They can all be summarized in the following table:

vertex	sliding line	figure	1	2	3
$H\phi\phi$	$\gamma, Z$	Fig. 33	$\phi$	$\phi$	$H$
	$Z$	Fig. 35	$\phi_z$	$\phi_z$	$\phi_z$
	$W^\pm$	Fig. 34	$\phi^\mp$	$\phi^\mp$	$\phi^\pm$
$H\phi_z\phi_z$	$W$	Fig. 33	$\phi_z$	$\phi$	$H$
	$W$	Fig. 35	$\phi_z$	$\phi$	$\phi_z$
	$Z$	Fig. 35	$\phi_z$	$\phi_z$	$\phi_z$
$HHH$	$W$	Fig. 35	$H$	$\phi$	$H$
	$Z$	Fig. 35	$H$	$\phi_z$	$H$

7. SSSS vertices:

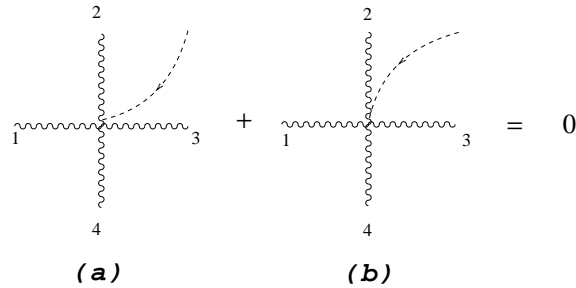


Figure 31: The cancellation of the  $gggg$  vertex.

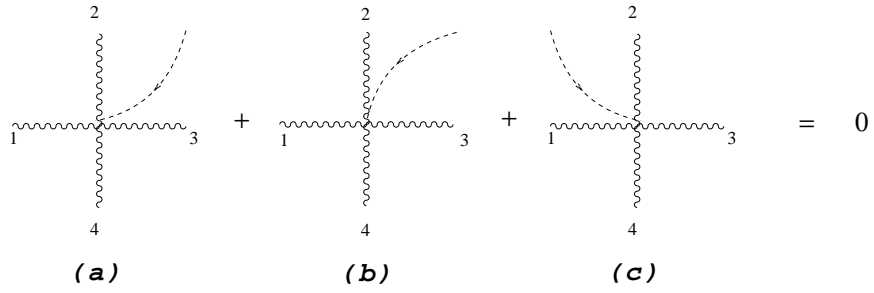


Figure 32: The cancellation of the  $ggg$  vertex.

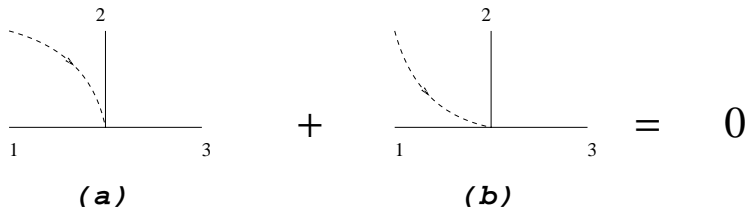


Figure 33: Cancellation relation of the  $SSS$  vertex.

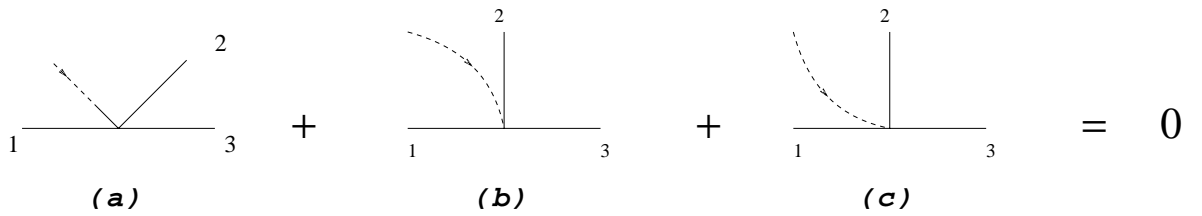


Figure 34: Cancellation relation of the  $SSS$  vertex.

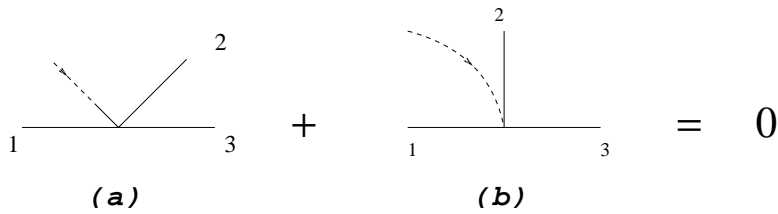


Figure 35: Cancellation relation of the  $SSS$  vertex.

(a)                      (b)

Figure 36: The cancellation relation of the  $SSSS$  vertex.

(a)                      (b)                      (c)

Figure 37: The cancellation relation of the  $SSSS$  vertex.

vertex	sliding line	figure	1	2	3	4
$\phi_z \phi_z \phi_z \phi_z$	$Z$	Fig. 37	$\phi_z$	$\phi_z$	$\phi_z$	$H$
	$W$	Fig. 37	$\phi_z$	$\phi_z$	$\phi_z$	$\phi$
$HHHH$	$Z$	Fig. 37	$\phi_z$	$H$	$H$	$H$
	$W$	Fig. 35	$\phi$	$H$	$H$	$H$
$\phi \phi \phi_z \phi_z$	$\gamma, Z$	Fig. 36	$\phi$	$\phi_z$	$\phi_z$	$\phi$
	$W$	Fig. 35	$\phi$	$\phi_z$	$\phi$	$\phi$
$HH\phi\phi$	$\gamma, Z$	Fig. 35	$\phi$	$H$	$H$	$\phi$
	$W^\pm$	Fig. 36	$\phi^\mp$	$\phi^\pm$	$H$	$\phi^\mp$
	$Z$	Fig. 35	$\phi$	$H$	$\phi_z$	$\phi$
$HH\phi_z\phi_z$	$W$	Fig. 37	$H$	$H$	$\phi$	$\phi_z$
$\phi\phi\phi\phi$	$\gamma, Z$	Fig. 35	$\phi$	$\phi$	$\phi$	$\phi$

(a)                      (b)                      (c)                      (d)

Figure 38: The cancellation relation of the  $SSSS$  vertex.

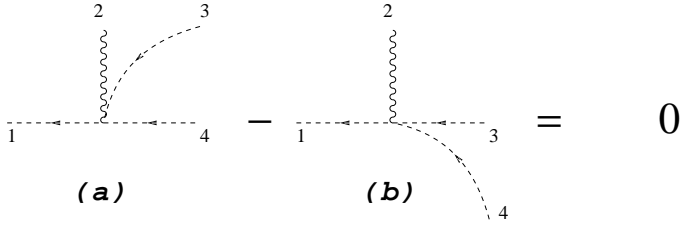


Figure 39: The cancellation relation of the  $gGG$  vertex.

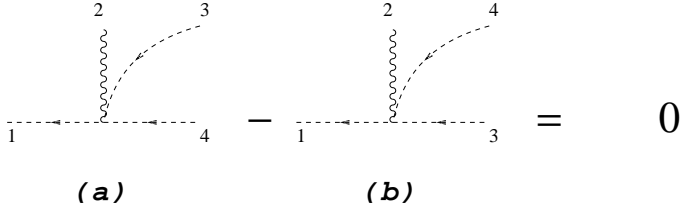


Figure 40: The cancellation relation of the  $gGG$  vertex.

8.  $gGG$ :

vertex	figure	1	2	3	4
$\bar{c}^\pm \gamma(Z) c^\mp$	Fig. 39	$c^\pm$	$W^\mp$	$c^+$	$c^-$
$\bar{c}^\pm \gamma(Z) c^\mp$	Fig. 40	$c^\pm$	$W^\mp$	$c^\mp$	$c^\mp$
$\bar{c}^\pm W^\mp c_\gamma(c_z)$	Fig. 40	$c^\pm$	$W^\mp$	$c_\gamma(c_z)$	$c_\gamma(c_z)$
$\bar{c}_\gamma(\bar{c}_z) W^\pm c^\mp$	Fig. 39	$\bar{c}_\gamma(\bar{c}_z)$	$W^\pm$	$c_\gamma(c_z)$	$c^\mp$

9.  $SGG$ : All the cancellations of this kind of vertices is represented by Fig. 41.

### B.3 Cancellation about the mass compensation diagrams

All of these have been considered in the above discussion.

## C GN gauge

### C.1 Divergence relations

First we look at the divergence relations of the vertices in the GN gauge. Since most of them are the same as those in the ordinary gauge, we just need to discuss those that are different.

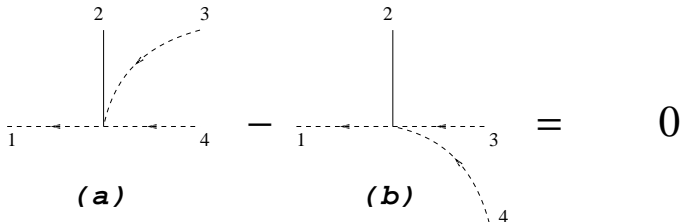


Figure 41: The cancellation relation of the  $SGG$  vertex.

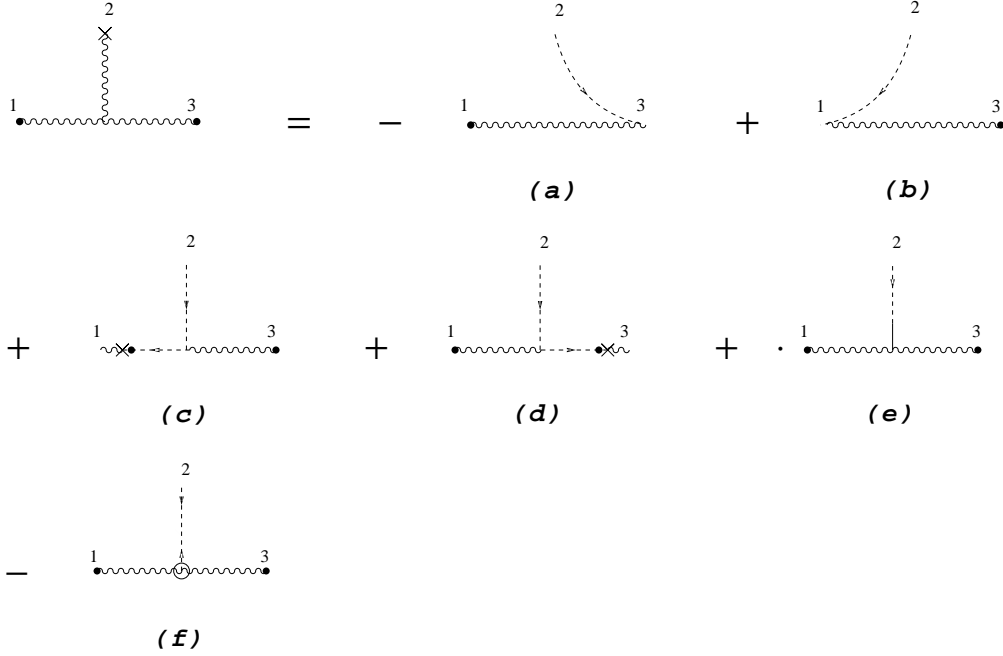


Figure 42: divergence relation of the triple gauge boson vertex in GN gauge.

1. ggg: It is shown in Fig. 42.

Here the extra diagram (f) is called *stagnant diagram* with a ghost line that can go nowhere.

2. gggg: We use the following table to summarize several cases:

Vertex	figure	1	2	3	4
$WWWW$	Fig. 43	$W$	$W$	$W$	$W$
$WW\gamma(Z)\gamma(Z)$	Fig. 43	$W$	$\gamma(Z)$	$W$	$\gamma(Z)$
$WW\gamma(Z)\gamma(Z)$	Fig. 44	$\gamma(Z)$	$W$	$\gamma(Z)$	$W$
$W\gamma WZ$	Fig. 44	$\gamma(Z)$	$W$	$Z(\gamma)$	$W$
$W\gamma WZ$	Fig. 43	$W$	$\gamma$	$W$	$Z$

3. gGG:

The divergence relation depends on whether the ghost vertex is a-type or b-type. The b-type ghost vertices have similar divergence relation as the charged scalar.

vertex	figure	1	2	3
$\bar{c}^- W^+ c_\gamma(c_z)$	Fig. 45	$c^-$	$W^+$	$c_\gamma(c_z)$
$\bar{c}^+ \gamma(Z) c^-$	Fig. 46	$c^+$	$\gamma(Z)$	$c^-$
$\bar{c}_\gamma(\bar{c}_z) W^- c^+$	Fig. 45	$\bar{c}_\gamma(\bar{c}_z)$	$W^-$	$c^+$

As for the a-type ghost vertices, they are cancelled according to the following table:

vertex	figure	line1	line2	line3	line4	$\lambda$
$W^- \bar{c}^+ c_\gamma(c_z)$	Fig. 47	$\bar{c}^+$	$\gamma(Z)$	$c^-$	$c_\gamma(c_z)$	1
	Fig. 47	$\bar{c}^+$	$W^-$	$c_\gamma(c_z)$	$c_\gamma(c_z)$	1
$\bar{c}_\gamma(\bar{c}_z) W^+ c^-$	Fig. 47	$\bar{c}_\gamma(\bar{c}_z)$	$W^+$	$c_\gamma(c_z)$	$c^-$	1
	Fig. 47	$\bar{c}_\gamma(\bar{c}_z)$	$\gamma(Z)$	$c^+$	$c^-$	1
$\bar{c}^- \gamma(Z) c^+$	Fig. 47	$\bar{c}^-$	$W^-$	$c^+$	$c^+$	0
	Fig. 47	$\bar{c}^-$	$W^+$	$c^-$	$c^+$	0



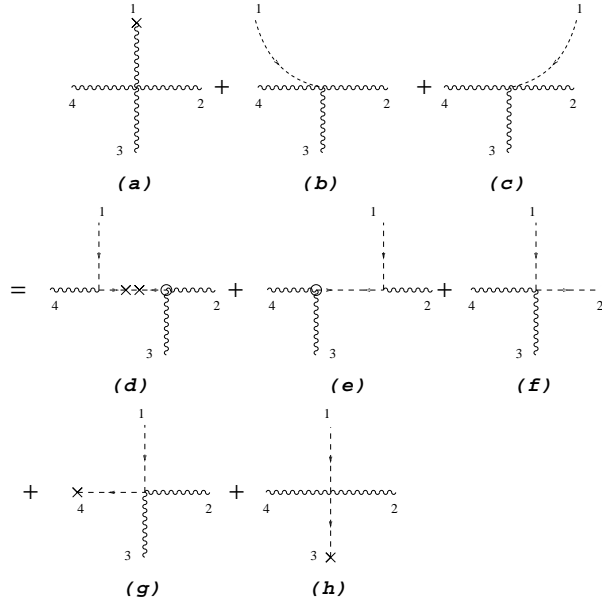


Figure 43: The divergence relation of the four gauge boson vertex in the GN gauge.

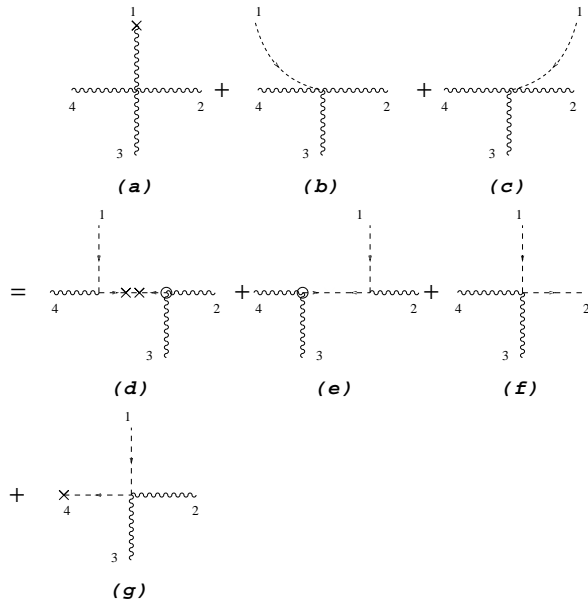


Figure 44: The divergence relation of the 4g-vertex in the GN gauge.

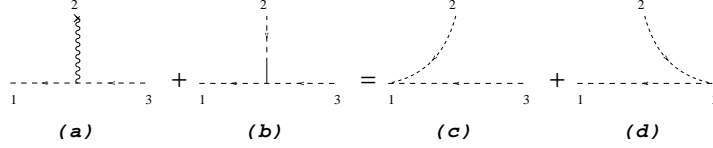


Figure 45: The divergence relation of the b-type ghost vertex in GN gauge.

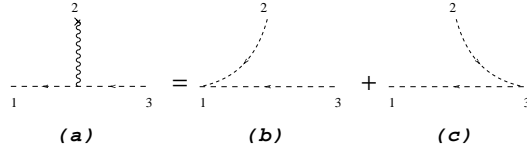


Figure 46: The divergence relation of the b-type ghost vertex in the GN gauge.

4. ggS: All the identities are the same as in Feynman gauge graphically, although now the vertices become those in GN gauge.

## C.2 Cancellation relations

1. ggg: They are contained in the discussion of the divergence relation of gggg above.
2. gggg: They are the same as in Feynman gauge, Although the gggg vertex has different expression.
3. gGG: All the possibilities of a ghost line being sliding into a gGG vertex are classified into the table below.

figure	line 1	line 2	line 3	line 4
Fig. 48	$\bar{c}^\pm$	$c^\mp$	$\gamma(Z)$	$c_\gamma(c_z)$
	$\bar{c}^\pm$	$c^\pm$	$c^\mp$	$W^\mp$
Fig. 49	$\bar{c}^\pm$	$c_\gamma(c_z)$	$c_\gamma(c_z)$	$W^{mp}$
	$\bar{c}^\pm$	$c^\mp$	$c^\mp$	$W^\pm$
	$\bar{c}_\gamma(\bar{c}_z)$	$c^+$	$c^-$	$\gamma(Z)$
Fig. 50	$\bar{c}_\gamma(\bar{c}_z)$	$c_\gamma(c_z)$	$c^\pm$	$W^\mp$

4. ggS: They are the same as in Feynman gauge, although the vertex factors are now different.

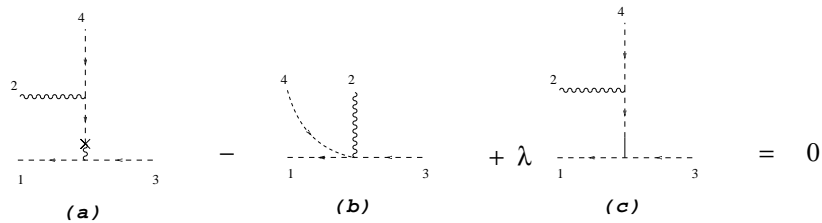


Figure 47: The divergence relation of the a-type ghost vertex.

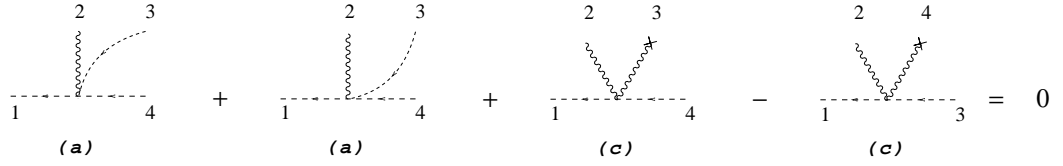


Figure 48: The cancellation relation of the  $gGG$  vertex in the GN gauge.

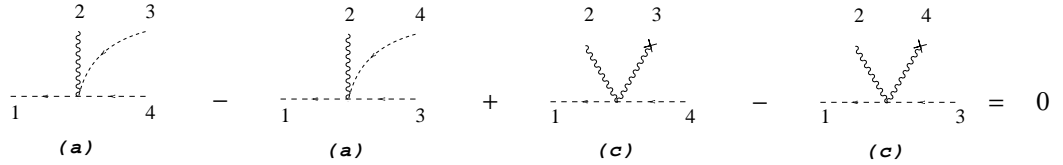


Figure 49: The cancellation relation of the  $gGG$  vertex in the GN gauge.

### 5. ggGG:

Since there are many possibilities here, we classify them in a new way. First if a ghost line slide to a ggGG vertex, we are then looking at a configuration with one outgoing ghost, two incoming ghosts, and two bosons. If those two ghost lines are the same, then any of them can be the wandering ghost line. These two cases just cancel each other. So in the following we just focus on the cases with different incoming ghost lines.

line 1	line 2	line 3	line 4	line 5	figure
$\bar{c}^+$	$c^-$	$c_\gamma(c_z)$	$\gamma(Z)$	$\gamma(Z)$	Fig. 51
$\bar{c}^-$	$c^+$	$c_\gamma(c_z)$	$\gamma(Z)$	$\gamma(Z)$	Fig. 52
$\bar{c}^+$	$c^+$	$c^-$	$W^-$	$\gamma(Z)$	Fig. 53
$\bar{c}^-$	$c^-$	$c^+$	$W^+$	$\gamma(Z)$	Fig. 51
$\bar{c}_\gamma(\bar{c}_z)$	$c_\gamma(c_z)$	$c^-$	$W^+$	$\gamma(Z)$	Fig. 54
$\bar{c}_\gamma(\bar{c}_z)$	$c_\gamma(c_z)$	$c^+$	$W^-$	$\gamma(Z)$	Fig. 55
$\bar{c}_\gamma(\bar{c}_z)$	$c^+$	$c^-$	$\gamma(Z)$	$\gamma(Z)$	Fig. 56

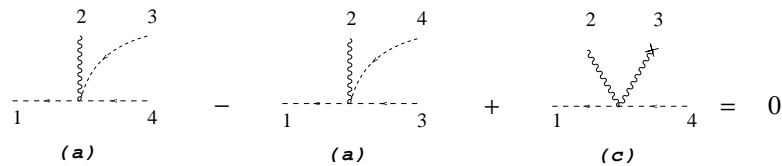


Figure 50: The cancellation relation of the  $gGG$  vertex in the GN gauge.

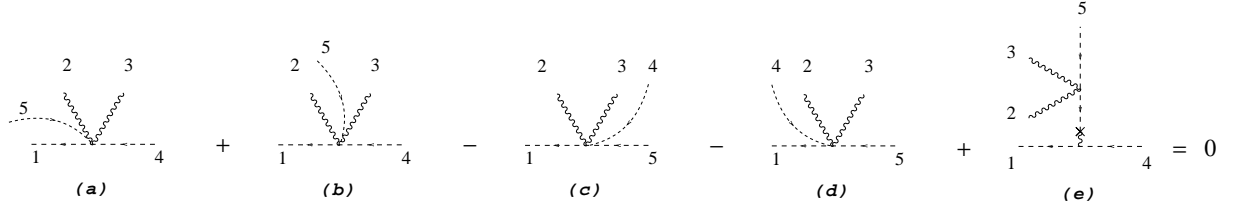


Figure 51: The cancellation relation of the  $ggGG$  vertex in the GN gauge.

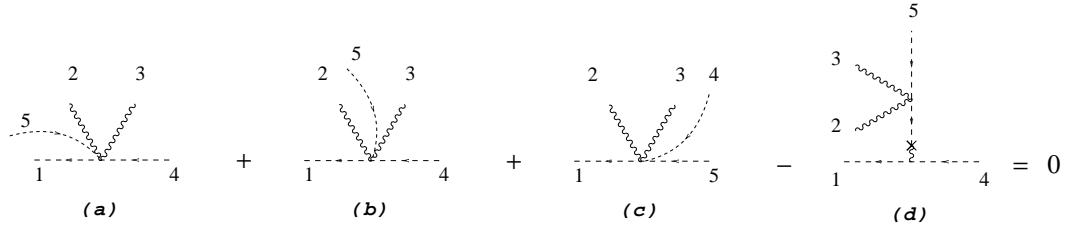


Figure 52: The cancellation relation of the  $ggGG$  vertex in the GN gauge.

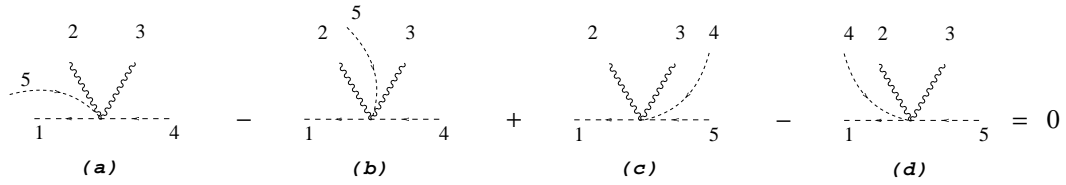


Figure 53: The cancellation relation of the  $ggGG$  vertex in the GN gauge.

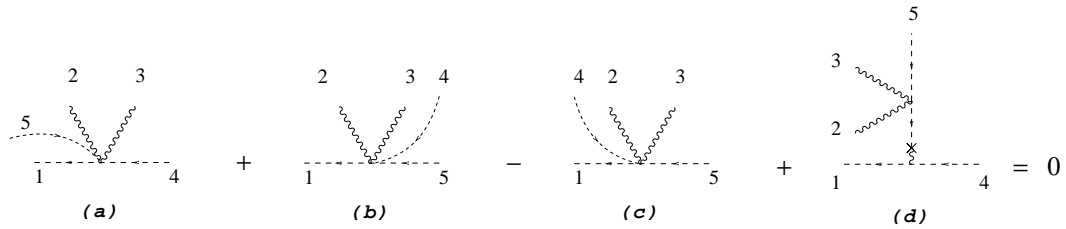


Figure 54: The cancellation relation of the  $ggGG$  vertex in the GN gauge.

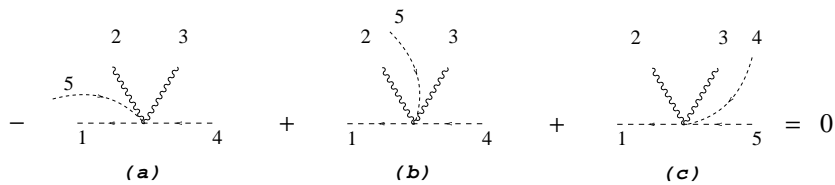


Figure 55: The cancellation relation of the  $ggGG$  vertex in the GN gauge.

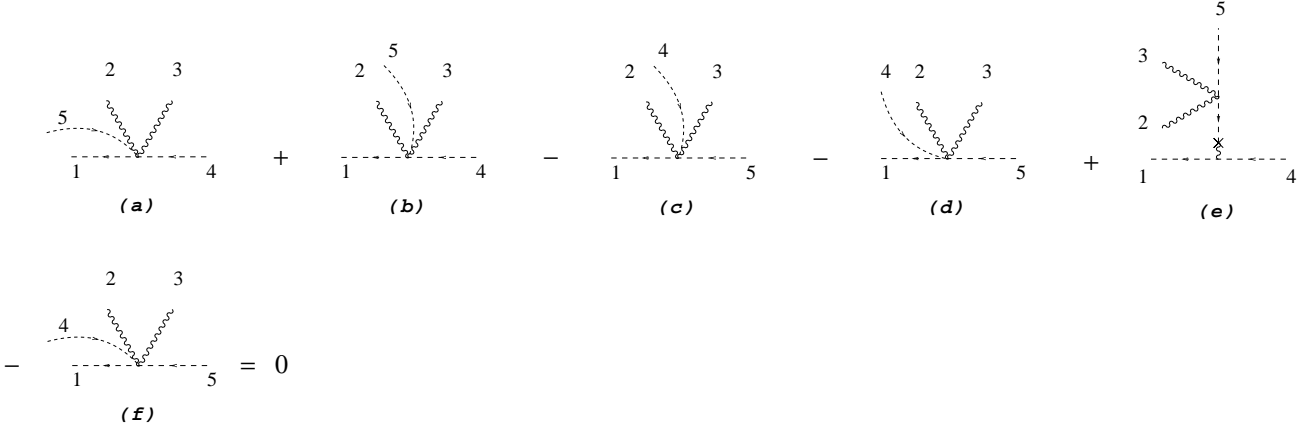


Figure 56: The cancellation relation of the  $ggGG$  vertex in the GN gauge.

## References

- [\*] e-mail address: feng@physics.mcgill.ca
- [†] e-mail address: lam@physics.mcgill.ca
- [1] Y.J. Feng and C.S. Lam, Phys. Rev **D53** (1996), 2115.
- [2] Y.J. Feng and C.S. Lam, to be published.
- [3] R. Gastmans, Tai Tsun Wu, *The Ubiquitous Photon: Helicity method for QED and QCD*, Clarendon Press (1990).  
M.L. Mangano, S.J. Parke, Phys. Rep. **200**, 301 (1991).
- [4] C.S. Lam and J.P. Lebrun, Nuovo Cimento A **59**, 397 (1969).  
C.S. Lam, Nucl. Phys. **B397**, 143 (1993).
- [5] Z. Bern and D.C. Dunbar, Nucl. Phys. **B379**, 562 (1992).  
Z. Bern and D.A. Kosower, Phys. Rev. Lett. **66**, 1669 (1991); Nucl. Phys. **B362**, 389 (1991); **B379**, 451 (1992).  
Z. Bern, L. Dixon, and D.A. Kosower, Phys. Rev. Lett. **70**, 2677 (1993).
- [6] M. Strassler, Nucl. Phys. **B385**, 145 (1992); SLAC preprint No. SLAC-PUB 5978, 1992 (unpublished).  
M.G. Schmidt and C. Schubert, Phys. Lett. B **331**, 69 (1994).
- [7] J.L. Gervais and A. Neveu, Nucl. Phys. **B46**, 381 (1972).
- [8] B.S. DeWitt, Phys. Rev. **162** (1967) 1195, 1239; in *Dynamic theory of groups and fields* (Gordon and Breach, 1965).  
G. 't Hooft, Nucl. Phys. **B62**, 444 (1973).  
L.F. Abbott, Nucl. Phys. **B185**, 189 (1981).
- [9] X. Li and Y. Liao, ASITP-94-50, hep-ph 9409401.  
A. Denner, G. Weiglein, and S. Dittmaier, hep-ph 9410338, Nucl. Phys. **B440**, 95 (1995).
- [10] J. Papavassiliou and K. Philippides, hep-ph 9503377; Phys. Rev. **D52** (1995), 2355;  
J. Papavassiliou and A. Pilaftsis, hep-ph 9506417, Phys. Rev. Lett. **75**, 3060 (1995).
- [11] G. Sterman, *Introduction to Quantum Field Theory*, Cambridge University Press 1993.
- [12] J.M. Cornwall, D.N. Levin, and G. Tiktopoulos, Phys. Rev. **D10** (1974), 1145;  
H.J. He, Yu-Ping Kuang, and C.-P. Yuan, YPI-IHEP-95-05, Phys.Rev. **D51** (1995), 6463.

The diagram illustrates an equation between two paths, (a) and (b), with an equals sign and a zero on the right. Path (a) consists of a horizontal dashed line from point 1 to point 4, a vertical solid line from point 4 to point 2, and a curved dashed line from point 2 to point 3. Path (b) consists of a horizontal dashed line from point 1 to point 3, a vertical solid line from point 3 to point 2, and a curved dashed line from point 2 to point 4. The labels (a) and (b) are centered below their respective paths.

$$(a) - (b) = 0$$

The diagram illustrates an equation involving three paths, labeled (a), (b), and (c), connected by minus and equals signs. Each path consists of a horizontal dashed line with arrows pointing left, a vertical solid line, and a curved dashed line.

- (a)**: The horizontal dashed line has endpoints labeled 1 and 4. The vertical solid line has its top endpoint labeled 2. The curved dashed line starts at the top of the vertical line and ends at a point labeled 3.
- (b)**: The horizontal dashed line has endpoints labeled 1 and 3. The vertical solid line has its top endpoint labeled 2. The curved dashed line starts at the top of the vertical line and ends at a point labeled 4.
- (c)**: The horizontal dashed line has endpoints labeled 1 and 3. The vertical solid line has its top endpoint labeled 2. The curved dashed line starts at the top of the vertical line and ends at a point labeled 4.

The equation is written as:  $(a) - (b) - (c) = 0$ .